J Supercond Nov Magn (2012) 25:961–968
DOI 10.1007/s10948-012-1403-x

ORIGINAL PAPER

A Study on Magnetoresistivity, Activation Energy, Irreversibility and Upper Critical Field of Slightly Mn Added Bi-2223 Superconductor Ceramics

M. Dogruer · Y. Zalaoglu · A. Varilci · C. Terzioglu · G. Yildirim · O. Ozturk

Received: 29 November 2011 / Accepted: 2 January 2012 / Published online: 14 January 2012

Abstract This study discusses the effect of Mn addition on the superconducting and physical properties in $Bi_{1.8}Pb_{0.4}Sr_2Mn_xCa_{2.2}Cu_{3.0}O_y$ bulk superconductors with $x = 0, 0.03, 0.06, 0.15, 0.3$, and 0.6 by means of the magnetoresistivity measurements. The magnetoresistivity of the samples prepared using the standard solid-state reaction method was measured for different values of the applied magnetic field strengths. The superconducting and physical properties of the samples such as the zero resistivity transition temperatures (T_c), irreversibility fields ($\mu_0 H_{irr}$), and upper critical fields ($\mu_0 H_{c2}$) were deduced from the magnetoresistivity curves. Moreover, thermally activated flux creep model was studied for activation energy (U_0) values of the samples. According to the results of the measurements, not only were the T_c and U_0 values of the samples found to decrease significantly but the $\mu_0 H_{irr}$ and $\mu_0 H_{c2}$ values were also observed to reduce with the increase in the Mn addition, indicating that the doping degrades the physical and superconducting properties of the samples.

Keywords $Bi_{1.8}Pb_{0.4}Sr_2Mn_xCa_{2.2}Cu_{3.0}O_y$ · Magnetoresistivity · Activation energy · Irreversibility field · Upper critical field

M. Dogruer (✉) · Y. Zalaoglu · A. Varilci · C. Terzioglu · G. Yildirim
Department of Physics, Abant Izzet Baysal University, Bolu 14280, Turkey
e-mail: musadogruer_23@hotmail.com

Y. Zalaoglu
Department of Physics, Osmaniye Korkut Ata University, Osmaniye 80000, Turkey

O. Ozturk
Department of Physics, Kastamonu University, Kastamonu 37100, Turkey

1 Introduction

During the discovery of high-temperature superconductor (HTSC) materials, scientists have endeavored to improve their superconducting, physical, mechanical, structural, and flux pinning properties to make them suitable for high temperature and magnetic field applications [1–3]. Bi-based (BSCCO) superconductors of the general formula $Bi_2Sr_2Ca_{n-1}Cu_nO_y$ ($n = 1, 2$, and 3) discovered in 1988 [4, 5] are the most promising materials for potential technological and industrial applications [6–12] due to the their remarkable smaller power losses, high current, and magnetic field carrying capacity, optical, and electronic properties [13–15]. The BSCCO system composed of a layered structure has three different phases with respect to its chemical compositions [16]. Among the phases, the Bi-2223 is the most attractive phase owing to the highest critical temperature (T_c) of about 110 K [17, 18]. On the other hand, its applications in high magnetic fields and temperatures are restricted because of the strong anisotropic property, very low charge carrier density, extremely short coherence length (ξ) and large penetration depth (λ), causing to unusually rapid flux creep which results in energy dissipation and subsequent transition of superconductor to the normal state [19]. Thus, the flux pinning mechanism investigated by Anderson [20], Kim [21], and Beasley et al. [22] in the superconducting state is a very useful tool for introduction of effective pinning centers such as planar defects, stacking faults, and microdefects, leading to thermally activated jumps,, or hopping of flux lines, or flux bundles over an energy barrier [23, 24]. Over the pinning energy barrier of a structure, the flux line can be thermally activated although the Lorentz force exerted on the flux bundle by the current is smaller than the pinning force. A model, described as thermally activated flux creep, works well in the resistivity region near T_c

($\rho = 0$) [25–28]. Furthermore, the width of the superconducting transition depends strongly on the anisotropy related to the orientation of the applied magnetic field with regard to the Cu–O planes in the structure [29–31]. Flux pinning ability can also be predicted from the flux pinning force density and activation energy values owing to the fact that the activation energy (mentioned as the potential barrier height) is generally regarded as a measure of flux pinning strength of a superconductor material [32–34]. The activation energy is determined from the thermally assisted flux creep theory described by Arrhenius equation $\rho = \rho_0 \exp(-U_0/k_B T)$, which will be explained in detail in results and discussion part.

In the present work, we investigated the effect of Mn doping on the superconducting and physical properties of the Bi-2223 ceramics by the magnetoresistivity measurements. The thermally activated flux creep model was adapted to fit the magnetoresistance curve under various applied magnetic field strengths in a range from 0 to 7 T. The superconducting transition temperatures, activation energies, irreversibility fields, and upper critical fields of the samples studied were determined with the aid of the model. According to the results, the superconducting and physical properties of the Bi-2223 superconductors were obtained to depend strongly on the Mn addition, representing the presence of magnetic ions. This phenomenon can be understood in terms of the pair-breaking mechanism [35], revealing the degradation of superconductivity and the exponential magnetic field dependence in the samples [36]. Moreover, the pair-breaking effect of nonmagnetic impurities is negligible in ordinary s-wave superconductors like BSCCO superconductors, whereas it can be large as in the case of magnetic impurities in usual s-wave superconductors. Thus, the addition or substitution of native ions by foreign ions in the BSCCO system results in a transition from a phase to another phase such as the superconductivity phase to semiconducting phase as a result of the pair-breaking mechanism.

2 Experimental Details

In this study, the superconducting and physical properties of Mn doped samples with nominal composition $Bi_{1.8}Pb_{0.4}Sr_2Mn_xCa_{2.2}Cu_{3.0}O_y$ ($x = 0, 0.03, 0.06, 0.15, 0.3,$ and 0.6) were investigated via the magnetoresistivity measurements. The samples produced in [37] were used for the aim of this work. The sample preparation procedure with the resistivity (ρ–T), transport critical current density (J_c), X-ray diffraction analysis (XRD), scanning electron microscopy (SEM), and electron dispersive X-ray (EDX) measurement results was given in detail elsewhere [37]. All the measurements were carried out using the zero field cooling (ZFC) procedure. The electrical resistivity versus temperature measurements were performed at various applied dc magnetic fields (0, 0.5, 1, 2, 4, and 7 T) at constant driving current of 5 mA. The magnetic fields generated from the superconducting coil magnet from CRYO Industries were applied normal to the direction of the driving current. Measurements were automated using GPIB interfaced by a personal computer. The measurement results obtained were recorded via the Labview computer software. The superconducting transition temperatures (T_c) of the samples prepared in this work were estimated from the magnetoresistivity measurements. Furthermore, activation energy values of the samples were determined by means of the line pinning model that calculates the energy by making linear fits to the low resistivity part of the transition [38–40]. Additionally, the irreversibility field ($\mu_0 H_{irr}$) and upper critical field ($\mu_0 H_{c2}$) were deduced from the resistivity versus the applied magnetic field curves. At a constant applied magnetic field, the temperature-dependent resistance is $R(\mu_0 H_{irr}, T) = 0.1 R_n$ for the $\mu_0 H_{irr}(T)$ field and $R(\mu_0 H_{c2}, T) = 0.9 R_n$ for the $\mu_0 H_{c2}(T)$ field, respectively. Here, R_n presents the normal state resistance of the samples at 130 K [41–45]. The samples will be herein after denoted as Mn0, Mn1, Mn2, Mn3, Mn4, and Mn5, respectively.

3 Results and Discussion

3.1 Magnetoresistivity Measurements

The temperature dependence of the resistivity in an external magnetic field ranging from 0 to 7 T for the Mn free and the Mn doped (Bi, Pb)-2223 samples prepared by the conventional solid-state reaction method was measured in the temperature range 50–130 K and the results obtained are depicted in Fig. 1. The electrical resistivity measurements were previously discussed in detail in [37]. Zero resistivity transition temperatures ($R = 0\ \Omega$) determined from Fig. 1 are given in Table 1. It is apparent from the table that the T of the samples studied gradually decreases from 109 K to 85 K at zero magnetic field ($\mu_0 H = 0$) as the Mn addition increases. The considerable decrement in the T_c value of the Mn5 sample is observed due to the decrease in the number of charge carriers in the sample [46].

Moreover, the variation of the transition temperatures determined under the applied magnetic field up to 7 T can be observed from Fig. 1. The transition temperatures obtained are listed in Table 1. It is visible from the table that the T_c value drastically decreases from 109 K to 66 K for the pure and 85 K to 36 K for the Mn5 sample with the increase of the applied magnetic field. The decrement in the T_c was found to be about 43 K and 49 K for the Mn0 and Mn5 sample, respectively. Based on these results, the zero resistivity transition temperature of the samples was noted to reduce dramatically with increasing both the Mn addition

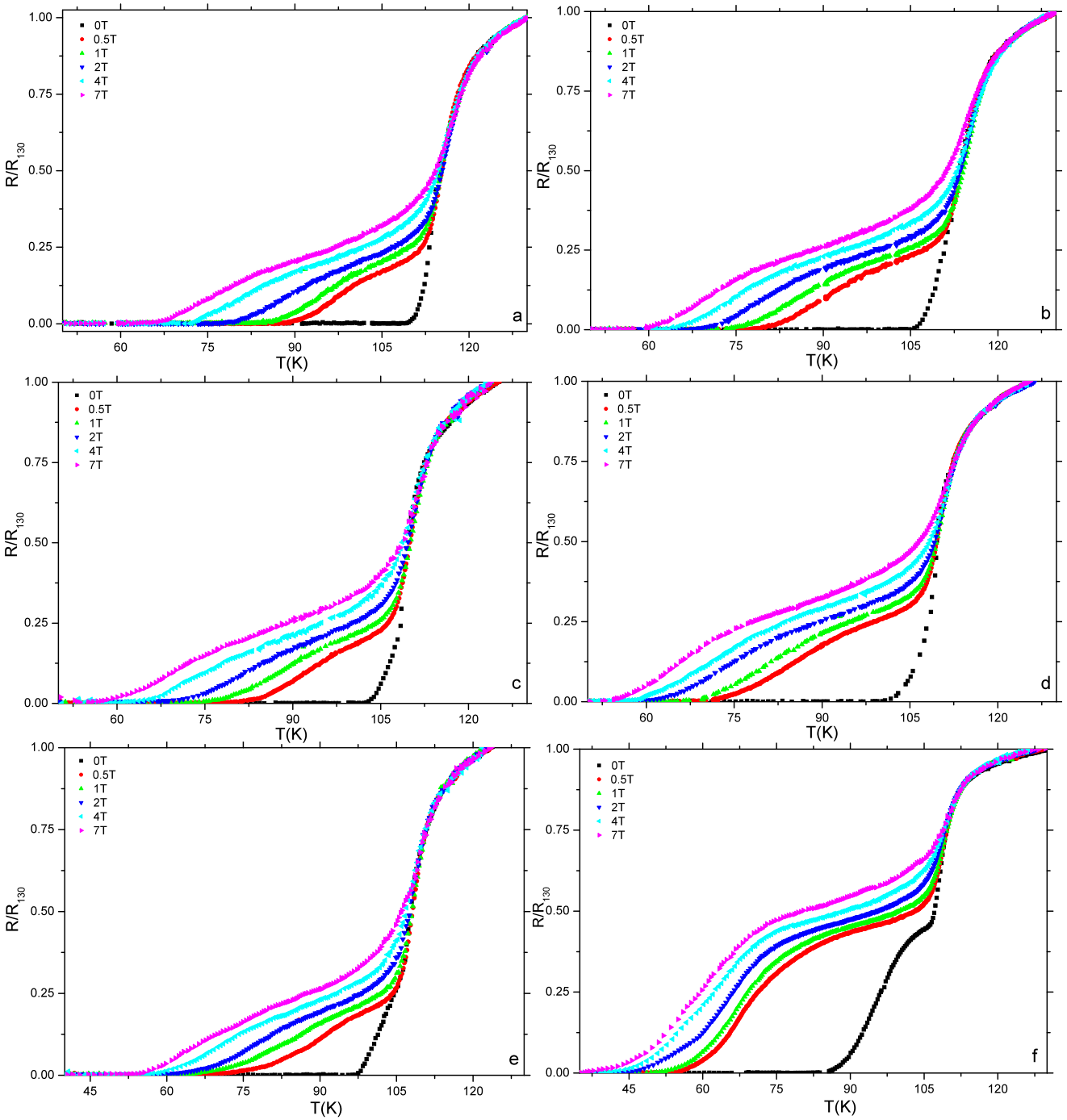

Fig. 1 ρ–T graphs of the samples at various magnetic field (0–7 T)

and applied magnetic field. It is well known that in all high-T_c ceramic superconductors, the CuO_2 planes containing the magnetic Cu^{2+} ions are the charge of superconductivity of the materials. Addition or substitution studies of 3d transition metal ions in the BSCCO system might lead to the sharp depression in critical temperature of the sample due to the replacement of Cu^{2+} ions by the foreign metal ions and so the Cu–O bond length is expanded in accordance with the increase of the lattice parameter a and decrease in the cell parameter c, causing to the suppression in the critical temperature of the samples. In this study, the Mn^{4+} ions penetrating into the Bi-2223 system degrade the pinning abilities and superconducting properties of the samples because of the pair breaking mechanism.

As well known from the literature, the onset critical temperature (T_c^{onset}) value is associated with the transition of

Table 1 Zero resistivity transition temperature (K) results of the samples under various applied magnetic fields

Samples	T_c^{onset} (K)	T_c^{offset} (K)					
		0 T	0.5 T	1 T	2 T	4 T	7 T
Mn0	118	109	88	85	78	72	66
Mn1	117	106	78	74	68	63	61
Mn2	115	103	75	72	65	62	58
Mn3	114	100	70	66	59	57	54
Mn4	113	98	67	63	57	56	52
Mn5	111	85	54	51	45	40	36

isolated grains to the superconducting state while the offset critical temperature (T_c^{offset}) is related to the volume fraction of Bi-2223 phase and/or features of intergranular component [47]. Hence, the applied magnetic field mostly affects the intergranular coupling of the cuprate superconductor materials and T_c^{onset} of a sample does not change significantly whereas T_c^{offset} decreases dramatically with the applied magnetic field due to the motion of fluxons [48, 49]. In this work, the broadening tail part of the resistivity curves was found to expand to lower temperature as the applied field increased, leading to the increase in the variation of $\Delta T_C (T_c^{onset} - T_c^{offset})$ value. As expected at 7 T applied magnetic filed, the minimum ΔT_c is observed to be about 52 K for the Mn0 whereas the maximum one is obtained to be about 75 K for the Mn5 sample (Table 1). According to the results, the T_c value of the samples prepared in this work was noticed to decrease considerably with the increase of both the Mn addition and applied magnetic field, associated with the decrease in the pinning force [50, 51]. In other words, the decreasing trend in pinning force of the samples with increasing Mn addition can be explained by the presence of impurities and weak links between the superconducting grains [3, 52].

3.2 Irreversibility and Upper Critical Field

The broadening of the resistivity transition under various applied magnetic fields was measured for determination of the irreversibility fields ($\mu_0 H_{irr}$) and upper critical fields ($\mu_0 H_{c2}$) of the samples at different temperature values. Tables 2 and 3 display the temperature dependence of $\mu_0 H_{irr}$ and $\mu_0 H_{c2}$ values obtained for all the samples. As seen from the tables, the $\mu_0 H_{irr}$ and $\mu_0 H_{c2}$ curves not only shift toward lower temperatures with the increase in the Mn addition but also enhance with the decrease of the temperature, confirming that the pinning ability of the Mn0 sample is stronger than that of others.

Table 2 Irreversibility field values of the samples

Samples	$\mu_0 H_{irr}(T)$					
	0 T	0.5 T	1 T	2 T	4 T	7 T
Mn0	110.878	92.023	88.412	82.19	74.371	69.357
Mn1	107.033	86.565	80.951	75.535	69.919	65.506
Mn2	105.094	83.64	78.823	73.408	67.39	63.178
Mn3	103.356	76.477	72.466	66.448	61.835	56.425
Mn4	98.37	69.895	66.707	59.937	52.716	47.978
Mn5	88.817	59.933	57.677	54.066	48.778	43.071

Table 3 Upper critical field values of the samples

Samples	$\mu_0 H_{c2}(T)$					
	0 T	0.5 T	1 T	2 T	4 T	7 T
Mn0	113.251	112.347	112.038	111.83	111.414	111.025
Mn1	111.045	110.486	109.632	109.021	108.504	108.258
Mn2	109.641	108.834	108.027	107.115	106.199	105.482
Mn3	107.772	106.764	105.757	104.945	103.128	101.914
Mn4	105.21	103.323	102.361	100.648	99.281	97.256
Mn5	100.876	98.617	96.906	94.344	92.283	90.800

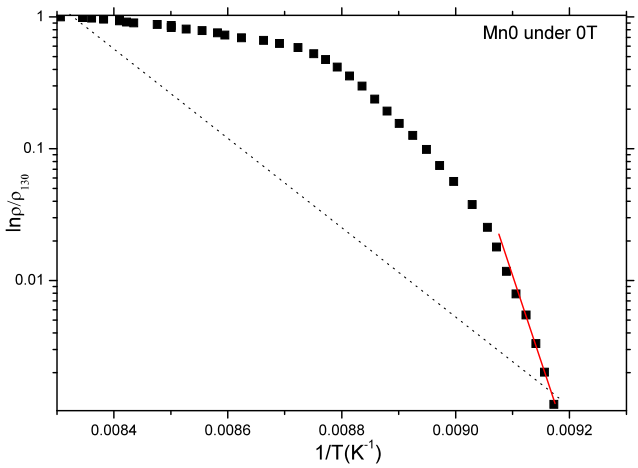

Fig. 2 The linear fit of the $\ln \rho/\rho_0$ versus $1/T$ graph for the Mn0 sample without any magnetic field (the *lines* are guides for the eye)

3.3 Activation Energy

Activation energy (U_0) plays an important role as the potential energy barrier to keep the magnetic flux in pinning center and the magnetoresistivity curves are also useful tool to determine the magnetic field dependence of the effective activation energy. Moreover, when the pinning force is sufficiently strong, vortex motion can be appeared small enough in the structure so that the superconductor acts as a perfect conductor. On the other hand, when the structure is exposed to strong currents, there will always be thermally activated

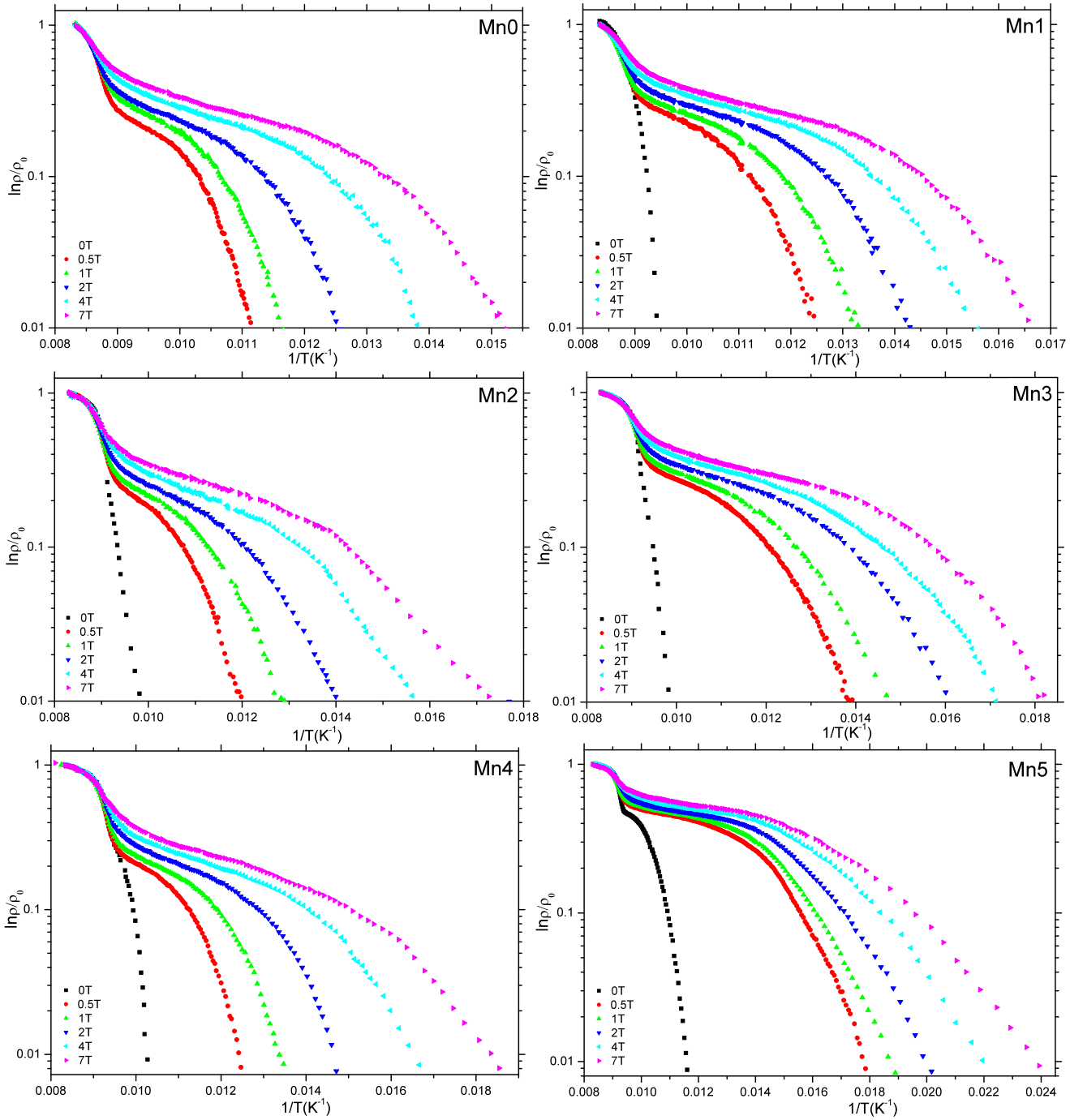

Fig. 3 $\ln \rho/\rho_0$ versus $1/T$ graphs of the samples. The activation energies of the samples are determined from the slopes of the linear parts of the low resistivity region

flux creep where vortices hop from one pinning site to an adjacent pinning site, and in some cases, we can measure the rate resulted from transition of the vortices [53–56]. In other words, thermally assisted flux creep is an essential dissipation mechanism resulting in a long resistive tail [57, 58] for the temperatures below the superconducting transition temperature. Thus, in this study the transport measurements were conducted instead of magnetic measurements to find more accurate activation energy values. The activation energies of the samples were deduced from the line pinning model by making linear fits to the low resistivity part of the transition. Namely, the variation of logarithmic resistivity as a function of the reciprocal of temperature for the samples at different applied magnetic fields is plotted and the activation

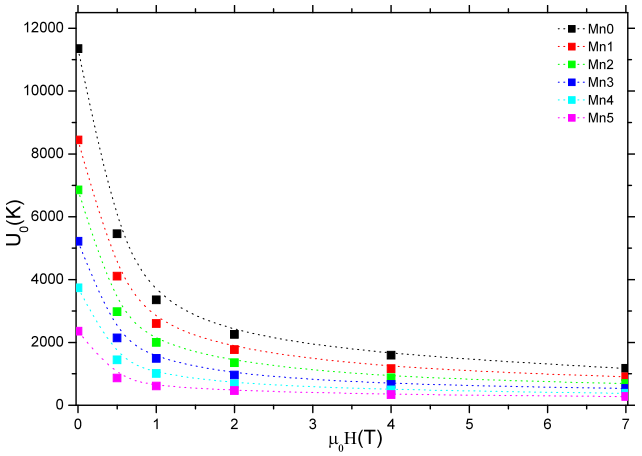

Fig. 4 Change of the activation energy values of the samples with the applied magnetic field up to 7 T

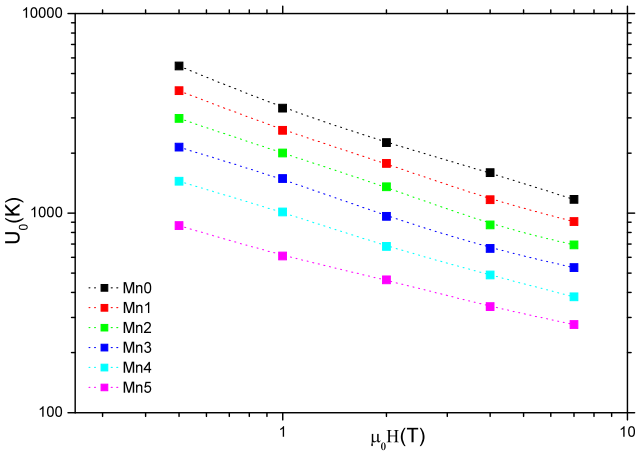

Fig. 5 Applied magnetic field dependence of activation energy (U_0) for the samples (the *lines* are guides for the eye)

energies are estimated from the slope of the linear part of the low resistivity region. Figure 2 shows that how we fit the $\ln \rho/\rho_0$ versus $1/T$ plot named as Arrhenius graph [59, 60]. As seen from the figure, the lines are guides for the eye and the slope of the straight line of the low resistivity region is assigned as the activation energy value. The Arrhenius plots of the magnetoresistivity data are given in Fig. 3. The results obtained from the semi logarithmic Arrhenius plots of Fig. 3 illustrate an exponential dependence of ρ with $1/T$, indicating that the energy dissipation (the resistivity) is due to the thermal activation of flux across the pinning barrier. The current-independent resistivity can be described by Arrhenius law [61–67], $\rho = \rho_0 \exp(-U_0/k_B T)$, where U_0 is the activation energy, k_B is the universal Boltzmann's constant and ρ_0 is a field-independent preexponential factor. For all the samples, the activation energies determined are shown in Fig. 4. It is visible from the figure that the activation energy values decrease drastically with the increase in both the Mn doping and applied magnetic field to a minimum (276 K) for the Mn5 sample as against 11350 K for the pure sample (Table 4) due to the decrement of the energy barriers in the samples. Additionally, all the samples produced have the same characteristic curve (Fig. 4) which decreases dramatically up to 1 T and then reduces slightly because of the fact that the applied magnetic field penetrates only the intergranular media below 1 T. Moreover, the samples prepared obtain different energy values at the same applied magnetic filed, pointing out the existence of various superconducting levels within the samples at the intergranular region [68–70]. According to these results, the Mn addition and applied field dependence of the activation energy may be consistent with the porosity, grain misorientations, and weak grain connectivity between the clusters in the samples, in agreement with the findings of [37]. This is probably the reason for decreases appearing in the flux pinning energy with increasing Mn addition.

Table 4 Activation energy and β values of the samples

Samples	Activation energies (K)						β values
	0 T	0.5 T	1 T	2 T	4 T	7 T	
Mn0	11350	5461	3497	2378	1676	1230	0.606
Mn1	8445	4107	2079	1520	1137	907	0.575
Mn2	6856	2979	1461	1069	828	693	0.551
Mn3	5214	2141	1130	853	665	553	0.526
Mn4	3740	1444	800	601	471	381	0.505
Mn5	2355	865	559	440	331	276	0.447

Moreover, we investigate the field dependence of the activation energy of the samples with the aid of the log–log plot of activation energy versus applied magnetic field (Fig. 5). The relation was noticed to be linear as seen in the figure and the field dependence of the activation energy can also be described by a power law as

$$U(H)\alpha H^{-\beta}. \quad (1)$$

When the data obtained from the measurements are fitted to (1), the β values are found to change in a range of 0.447–0.606 (Table 4). The minimum β value was found to be about 0.447 for the Mn5 sample whereas the maximum value was observed to be about 0.606 for the pure sample, confirming that the activation energy is related to the plastic deformation of flux line lattice at dislocations, similar to the thermally activated motion of edge dislocations in crystals [71, 72]. In the literature, for the BSCCO-2212 system [73] and the BSCCO-2223 system [74, 75], the field dependence of the activation energy is obtained to be about 0.5.

4 Conclusion

This study aims to analyze the role of Mn addition on the superconducting and physical properties of (Bi,Pb)-2223 su-

perconductors with the aid of the magnetoresistivity measurements. The zero resistivity transition temperatures, activation energies, irreversibility fields, and upper critical fields were determined from the R–T curves under dc magnetic fields up to 7 T. It was found that the T_c and U_0 values of the samples were predominately dependent upon the Mn addition. The minimum T_c of 40 K and U_0 of 276 K at 7 T applied magnetic field were obtained for Mn5 sample. Based on these results, the pinning abilities, the superconducting, and physical properties of the Bi-2223 superconductor ceramics produced in this work were found to decrease with the increase of the Mn addition due to the pair-breaking mechanism.

Acknowledgements This study is dedicated to his newborn daughter of Alpaslan Karabulut.

References

1. Ghazanfari, N., Kilic, A., Gencer, A., Ozkana, H.: Solid State Commun. **144**, 210 (2007)
2. Makise, T., Uchida, S., Horii, S., Shimoyama, J., Kishio, K.: Physica C **460–462**, 772 (2007)
3. Yildirim, G., Zalaoglu, Y., Akdogan, M., Altintas, S.P., Varilci, A., Terzioglu, C.: J. Supercond. Nov. Magn. **24**, 2153 (2011)
4. Maeda, H., Tanaka, Y., Fukutomi, M., Asano, T.: Jpn. J. Appl. Phys. Lett. **27**, L209 (1988)
5. Tarascon, J.M., Lepage, Y., Greene, L.H., Bagley, B.G., Barboux, P., Hwang, D.M., Hull, G.W., Makinnon, W.R., Giroud, M.: Phys. Rev. B **38**, 2504 (1988)
6. Tsukamoto, A., Imagawa, K., Hiratani, M., Kanehori, K., Takagi, K.: Jpn. J. Appl. Phys. **30**, L830 (1991)
7. Jannah, A.N., Halim, S.A., Abdullah, H.: Eur. J. Sci. Res. **29**, 438 (2009)
8. Hakuraku, V., Mori, Z., Oku, S.: Supercond. Sci. Technol. **6**, 408 (1993)
9. Yildirim, G., Akdogan, M., Altintas, S.P., Erdem, M., Terzioglu, C., Varilci, A.: Physica B **406**, 1853 (2011)
10. Aksan, M.A., Yakinci, M.E., Guldeste, A.: Thin Solid Films **515**, 8022 (2007)
11. Martinez, H., Marino, A., Rodriguez, J.E.: Physica C **408–410**, 568 (2004)
12. Aksan, M.A., Altin, S., Yakinci, M.E., Guldeste, A., Balci, Y.: Mater. Sci. Technol. **27**, 314 (2011)
13. Runde, M.: IEEE Trans. Appl. Supercond. **5**, 813 (1995)
14. Godeke, A., Cheng, D., Dietderich, D.R., English, C.D., Felice, H., Hannaford, C.R., Prestemon, S.O., Sabbi, G., Scanlan, R.M., Hikichi, Y., Nishioka, J., Hasegawa, T.: IEEE Trans. Appl. Supercond. **18**, 516 (2008)
15. Miao, H., Meinesz, M., Czabai, B., Parrell, J., Hong, S.: AIP Conf. Proc. **986**, 423 (2008)
16. Mousavi Ghahfarokhi, S.E., Zargar Shoushtari, M.: Physica B **405**, 4643 (2010)
17. Sarkar, K.A., Maartense, I., Peterson, T.L., Kumar, B.: J. Appl. Phys. **66**, 3717 (1989)
18. Rhee, C.K., Kim, C.J., Lee, H.G., Kuk, I.H., Lee, J.M., Chang, I.S., Rim, C.S., Han, P.S., Pyun, S.I., Won, D.Y.: Jpn. J. Appl. Phys. **28**, L1137 (1989)
19. Sarun, P.M., Vinu, S., Shabna, R., Biju, A., Syamaprasad, U.: Mater. Res. Bull. **44**, 1017–1021 (2009)
20. Anderson, P.W.: Phys. Rev. Lett. **9**, 309 (1962)
21. Anderson, P.W., Kim, Y.B.: Rev. Mod. Phys. **36**, 39 (1964)
22. Beasley, M.R., Labusch, R., Webb, W.W.: Phys. Rev. **181**, 682 (1969)
23. Ishida, T., Mazaki, H.: Phys. Rev. B **20**, 131–138 (1979)
24. Pande, C.S., Masumura, R.A.: Physica C **314**, 147 (1999)
25. Palstra, T.T., Batlogg, B., Schneemeyer, L.F., Waszczak, J.V.: Phys. Rev. Lett. **61**, 662 (1988)
26. Malozemoff, A.P., Worthington, T.K., Zeldov, E., Yeh, N.C., McElfresh, M.W.: In: Fukuyama, H., Maekawa, S., Malozemoff, A.P. (eds.) Strong Correlation and Superconductivity. Springer Series in Sol. State Sci., vol. 89. Springer, Berlin (1989)
27. Griessen, R.: Phys. Rev. Lett. **64**, 1674 (1990)
28. Ma, R.C., et al.: Physica C **405**, 34 (2004)
29. Charalambous, M., Chaussy, J., Lejay, P.: Phys. Rev. B **45**, 5091 (1992)
30. Xu, X.J., Fu, L., Wang, L.B., Zhang, Y.H., Fang, J., Cao, X.W., Li, K.B., Hisashi, S.: Phys. Rev. B **59**, 608 (1999)
31. Salem, A., Jakob, G., Adrian, H.: Physica C **402**, 354 (2004)
32. Wan, X., Sun, Y., Song, W., Jiang, L., Wang, K., Du, J.: Supercond. Sci. Technol. **11**, 1079 (1998)
33. Vinu, S., Sarun, P.M., Shabna, R., Syamaprasad, U.: J. Alloys Compd. **487**, 1 (2009)
34. Pu, M.H., Song, W.H., Zhao, B., Wu, X.C., Sun, Y.P., Du, J.J., Fang, J.: Physica C **361**, 181 (2001)
35. Coskun, A., Ekicibil, A., Ozcelik, B.: Chin. J. Phys. **43**, 372 (2005)
36. Lay, L.L., Friend, C.M., Maruyama, T., Osamura, K., Hampshire, D.P.: J. Phys., Condens. Matter **6**, 10053 (1994)
37. Yildirim, G., Bal, S., Yucel, E., Dogruer, M., Akdogan, M., Varilci, A., Terzioglu, C.: J. Supercond. Nov. Magn. (2011). doi:10.1007/s10948-011-1324-0
38. Smith, G.B., Bell, J.M., Filipczuk, S.W., Andrikidis, C.: Physica C **160**, 333 (1989)
39. Inui, M., Littlewood, P.B., Coppersmith, S.N.: Phys. Rev. Lett. **63**, 2421 (1989)
40. Vo, N.V., Liu, H.K., Dou, S.X.: Supercond. Sci. Technol. **9**, 104 (1996)
41. Ososky, M.S., Soulen, R.J., Wolf, S.A., Broto, J.M., Rakoto, J.M., Ousset, J.C., Coffe, G., Askenazy, S., Pari, P., Bozovic, I., Eckstein, J.N., Virshup, G.F.: Phys. Rev. Lett. **71**, 2315 (1993)
42. Kim, J.H., Dou, S.X., Shi, D.Q., Rindfleisch, M., Tomsic, M.: Supercond. Sci. Technol. **20**, 1026 (2007)
43. Erdem, M., Ozturk, O., Yucel, E., Altintas, S.P., Varilci, A., Terzioglu, C., Belenli, I.: Physica B **406**, 705 (2011)
44. Kitaguchi, H., Matsumoto, A., Hatakeyama, H., Kumakura, H.: Supercond. Sci. Technol. **17**, S486 (2004)
45. Yadav, C.S., Paulose, P.L.: New J. Phys. **11**, 103046 (2009)
46. Yildirim, G., Yucel, E., Bal, S., Dogruer, M., Varilci, A., Akdogan, M., Terzioglu, C., Zalaoglu, Y.: J. Supercond. Nov. Magn. (2011). doi:10.1007/s10948-011-1284-4
47. Yazici, D., Erdem, M., Ozcelik, B.: J. Supercond. Nov. Magn. (2011). doi:10.1007/s10948-011-1331-1
48. Bhalla, G.L., Malik Pratima, A., Singh, K.K.: Physica C **391**, 17 (2003)
49. Moodera, J.S., Meservey, R., Tkaczyk, J.E., Hao, C.X., Gibson, G.A., Tedrow, P.M.: Phys. Rev. B **37**, 619 (1988)
50. Tinkham, M.: Introduction to Superconductivity, 2nd edn. McGraw-Hill, New York (1996)
51. Ozkurt, B., Ozcelik, B.: J. Low Temp. Phys. **156**, 22–29 (2009)
52. Liyanawaduge, N.P., Kumar, A., Kumar, S., Karunarathne, B.S.B., Awana, V.P.S.: J. Supercond. Nov. Magn. (2011). doi:10.1007/s10948-011-1203-8
53. Yildirim, G., Bal, S., Yucel, E., Dogruer, M., Akdogan, M., Varilci, A., Terzioglu, C.: J. Supercond. Nov. Magn. (2011). doi:10.1007/s10948-011-1324-0
54. Wang, Y., Wen, H.H.: Europhys. Lett. **81**, 57007 (2008)

55. Chen, X.J., Struzhkin, V., Wu, Z., Lin, H.Q., Hemley, R.J., Mao, H.K.: Proc. Natl. Acad. Sci. USA **104**, 3732 (2007)
56. Olson, C.J., Reichhardt, C., Nori, F.: Phys. Rev. B **56**, 6175–6194 (1997)
57. Kusevic, I., Babic, E., Marohnic, Z., Ivkov, J., Liu, H.K., Dou, S.X.: Physica C **235–240**, 3035 (1993)
58. Liu, H.K., Guo, Y.C., Dou, S.X., Cassidy, S.M., Cohen, L., Perkins, G.K., Caplin, A.D.: Physica C **213**, 95 (1993)
59. Kucera, J.T., Orlando, T.P., Virshup, G., Eckstein, J.N.: Phys. Rev. B **46**, 11004 (1992)
60. Yamasaki, H., Endo, K., Kosaka, S., Umeda, M., Yoshida, S., Kajimura, K.: Phys. Rev. Lett. **70**, 3331 (1993)
61. Abou-Aly, A.I., Mostafa, M.F., Ibrahim, I.H., Awad, R., Al-Hajji, M.A.: Supercond. Sci. Technol. **15**, 938 (2002)
62. Batista-Laeyva, A.J., Cobas, R., Orlando, M.T.D., Altshuler, E.: Supercond. Sci. Technol. **16**, 857 (2003)
63. Sung, H.H., Yang, H.C., Chen, H.C., Horng, H.E., Yao, B.C.: Chin. J. Phys. **30**, 247 (1992)
64. Attanasio, C., Salvato, M., Ciancio, R., Gombos, M., Pace, S., Uthayakumar, S., Vecchione, A.: Physica C **411**, 126 (2004)
65. Govea-Alcaide, Es., Hernandez-Wolpez, M., Batista-Leyva, A.J., Jardim, R.F., Mune, P.: Physica C **423**, 51 (2005)
66. Passos, C.A.C., Orlando, M.T.D., Fernandes, A.A.R., Oliveira, F.D.C., Simonetti, D.S.L., Fardin, J.F., Belich, H. Jr, Ferreira, M.M. Jr: Physica C **419**, 25 (2005)
67. Pu, M.H., Feng, Y., Zhang, P.X., Wang, J.X., Du, J.J., Zhou, L.: Physica C **412–414**, 467 (2004)
68. Govea-Alcaide, E., Garcia-Fornaris, I., Mune, P., Jardim, R.F.: Eur. Phys. J. B **58**, 373 (2007)
69. Muné, P., Govea-Alcaide, E., Jardim, R.F.: Physica C **384**, 491 (2003)
70. Albrecht, J., Jooss, Ch., Warthmann, R., Forkl, A., Kronmüller, H.: Phys. Rev. B **57**, 10332 (1998)
71. Geshkenbein, V., Larkin, A., Feigelman, M., Vinokur, V.: Physica C **162–164**, 239 (1989)
72. Paradhan, A.K., Muralidhar, M., Feng, Y., Murakami, M., Nakao, K., Koshizuka, N.: Phys. Rev. B **64**, 172505 (2001)
73. Noetzel, R., Westerholt, K.: Phys. Rev. B **58**, 15108 (1998)
74. Soulen, R.J. Jr., Wolf, S.A.: Physica C **1–2**, 95 (1990)
75. Yildirim, G., Dogruer, M., Ozturk, O., Varilci, A., Terzioglu, C., Zalaoglu, Y.: J. Supercond. Nov. Magn. (2011). doi:10.1007/s10948-011-1384-1